SAE International

2012-01-1285
Published 04/16/2012

doi:10.4271/2012-01-1285
saefuel.saejournals.org

Effects of Combustion Phasing, Injection Timing, Relative Air-Fuel Ratio and Variable Valve Timing on SI Engine Performance and Emissions using 2,5-Dimethylfuran

Ritchie Daniel, Chongming Wang and Hongming Xu
University of Birmingham

Guohong Tian
Newcastle University

ABSTRACT

Ethanol has long been regarded as the optimal gasoline-alternative biofuel for spark-ignition (SI) engines. It is used widely in Latin and North America and is increasingly accepted as an attractive option across Europe. Nevertheless, its low energy density requires a high rate of manufacture; in areas which are deficient of arable land, such rates might prove problematic. Therefore, fuels with higher calorific values, such as butanol or 2,5-dimethylfuran (DMF) deserve consideration; a similar yield to ethanol, in theory, would require much less land. This report addresses the suitability of DMF, to meet the needs as a biofuel substitute for gasoline in SI engines, using ethanol as the biofuel benchmark. Specific attention is given to the sensitivity of DMF to various engine control parameters: combustion phasing (ignition timing), injection timing, relative air-fuel ratio and valve timing (intake and exhaust). Focus is given to the window for optimization; the parameter range which sustains optimal IMEP (within 2%) but provides the largest reduction of emissions (HC or NO_x). The test results using a single cylinder SI research engine at 1500rpm show how DMF is less sensitive to key engine parameters, compared to gasoline. This allows a wider window for emissions optimization because the IMEP remains optimal across a greater parameter range.

CITATION: Daniel, R., Wang, C., Xu, H. and Tian, G., "Effects of Combustion Phasing, Injection Timing, Relative Air-Fuel Ratio and Variable Valve Timing on SI Engine Performance and Emissions using 2,5-Dimethylfuran," *SAE Int. J. Fuels Lubr.* 5(2):2012, doi:10.4271/2012-01-1285.

INTRODUCTION

With ever-increasing concerns over fuel security and the problem of global warming, there is a greater need to pursue alternative energy sources. Carbon-free fuels, which do not emit carbon dioxide (CO_2) once consumed, are the long-term ideal in order to eradicate carbon emissions. However, biofuels offer a short- to mid-term solution in reducing the dependence on mineral oil and overall, or life-cycle CO_2 emissions.

One particular biofuel candidate, which can help to reduce life-cycle CO_2 emissions is 2,5-dimethylfuran, otherwise known as DMF. In 2007, bioscientists at the University of Wisconsin-Madison publicized technological breakthroughs in its manufacture and the production of high yields [1, 2]. Since then, these techniques have benefitted from further iterations by other institutions [3,4,5,6,7]. These developments have attracted the attention from automotive researchers in the potential use of DMF as an alternative energy carrier to gasoline. In comparison to ethanol, DMF offers several improvements, including a higher energy density (approximately 40% higher) and insolubility in water [8].

Currently, relatively few publications exist on DMF as a gasoline-alternative fuel. The first reported engine studies were conducted by the authors' group [9,10,11]. This added to the laboratory studies of the laminar burning velocity [12,13,14,15], spray properties [16] and combustion intermediates of DMF [17] from the authors (summarized in an online book chapter [18]) and collaborating Chinese universities. Evidently, this publication contributes to a series of experiments led by the authors' group to explore the use of DMF as a fuel for automotive applications.

One such area to explore is the sensitivity of DMF to various engine parameters. The sensitivity of a fuel to engine parameters affects the ability to optimize the engine for

various emissions and efficiency trade-offs. The most influential parameter in a spark-ignition (SI) engine is the ignition timing. This significantly affects the combustion process, which determines the fuel economy, torque output and emissions performance [19]. Usually, the ignition timing is optimized using sophisticated mathematical approaches, including advanced Design of Experiment (DoE) methodologies [20,21,22], in order to find the optimum, or minimum advance for best torque (MBT) timing. Minimal advance or retard about this point gives modest variation in power and fuel consumption but can lead to large changes in NO_x and HC emissions. Clearly, an alternative fuel which produces the largest reduction in emissions, whilst achieving competitive performance has the greatest value in a practical application.

Another engine control parameter which dramatically influences the combustion behavior in modern direct-injection (DI) engines is the injection timing. The injection timing can help to reduce the fuel consumption at low and part-load through stratification, as the pumping losses are reduced [23]. Alternatively, at high-load, the engine torque can be increased due to charge-cooling as the knock is suppressed and the ignition timing can be advanced. The much higher injection pressures of DI also encourages rapid fuel atomization and an increased vaporization rate, which also aids combustion stability [24]. However, this can lead to fuel impingement on the piston or cylinder wall [25]. Therefore, as with ignition timing, it is essential to understand the change in engine behavior as the injection timing is varied when introducing new fuels. Each fuel has a different impact on the charge-cooling and the particle size distribution will affect the extent of vaporization and wall wetting. Ethanol is highly sensitive to the injection timing due to the high latent heat of vaporization [26, 27]. Although this can help to increase maximum IMEP, it does narrow the window for emissions optimization for a given performance drop from the optimum.

The use of stratified or lean combustion has become commonly applied to modern direct-injection spark-ignition (DISI) engines [28]. This is a method to simultaneously increase efficiency and reduce emissions but is also very complex to control [29]. At part-load operation the greater throttle opening reduces the pumping losses usually associated with stoichiometric operation. In terms of emissions, lean-burn strategies can also dramatically reduce nitrous oxide (NO_x) emissions, as the production of NO_x is very temperature dependant. This lean burn option becomes more possible because of the development of high conversion efficiency NO_x traps [30]. Nevertheless, as the mixture is leaned, the combustion approaches the limit of stable operation. At this 'lean limit', the ignition becomes unreliable and complete combustion is unsustainable, resulting in engine misfire [31]. Such a lean limit is also fuel dependant because the vaporization rates and combustion speeds vary. Therefore, a fuel which produces a very lean combustion limit will enable a wide window for optimization and provides an opportunity to greatly reduce NO_x emissions.

With more alternative fuels being investigated in the search for fossil fuel replacements, it is important to fully understand their combustion characteristics. This paper investigates the difference in several parameter sensitivities to engines that are fuelled with ethanol and DMF. Such parameters include: ignition timing, injection timing, air-fuel ratio (AFR) and valve timing (intake and exhaust). Apart from the variation of ignition timing, the parameters were mainly tested at high load (8.5bar IMEP). Sweeps were conducted around the reference operating condition and the change in load and other parameters was observed. At the highest load condition, clearer separations occur between the fuels. Also, where the effect on emissions is analyzed, only the NO_x and total hydrocarbon (HC) emissions have been investigated. In the following sections, the engine setup, experimental results and finally conclusions are discussed.

EXPERIMENTAL SETUP

In this section the experimental setup and procedure are discussed in turn, as similarly found in a previous publication by the authors [11]. However, in this work, more emphasis is placed on the method of performing the individual parameter sweeps.

ENGINE AND INSTRUMENTATION

The experiments were performed on a single-cylinder, 4-stroke SI research engine, as shown in Figure 1. The 4-valve cylinder head includes the Jaguar spray-guided DISI technology used in their V8 production engine (AJ133) [32]. It also includes variable valve timing technology for both intake and exhaust valves.

The engine was coupled to a DC dynamometer to maintain a constant speed of 1500±1rpm, regardless of the torque output. The in-cylinder pressure was measured using a Kistler 6041A water-cooled pressure transducer which was fitted flush to the side-wall of the cylinder head. The signal was then passed to a Kistler 5011 charge amplifier and finally to a National Instruments data acquisition card. Samples were taken at 0.5CAD intervals for 300 consecutive cycles, so that an average could be taken. The crankshaft position was measured using a digital shaft encoder mounted on the crankshaft. Coolant and oil temperatures were controlled at 85±5°C and 95±3°C respectively using a Proportional Integral Differential (PID) controller. All temperatures were measured with K-type thermocouples.

The engine was controlled using software developed in-house written in the LabVIEW programming environment. High-speed, crank-angle-resolved and low-speed, time-resolved data was also acquired using LabVIEW. This was then analyzed using MATLAB developed code so that an analysis of the combustion performance could be made.

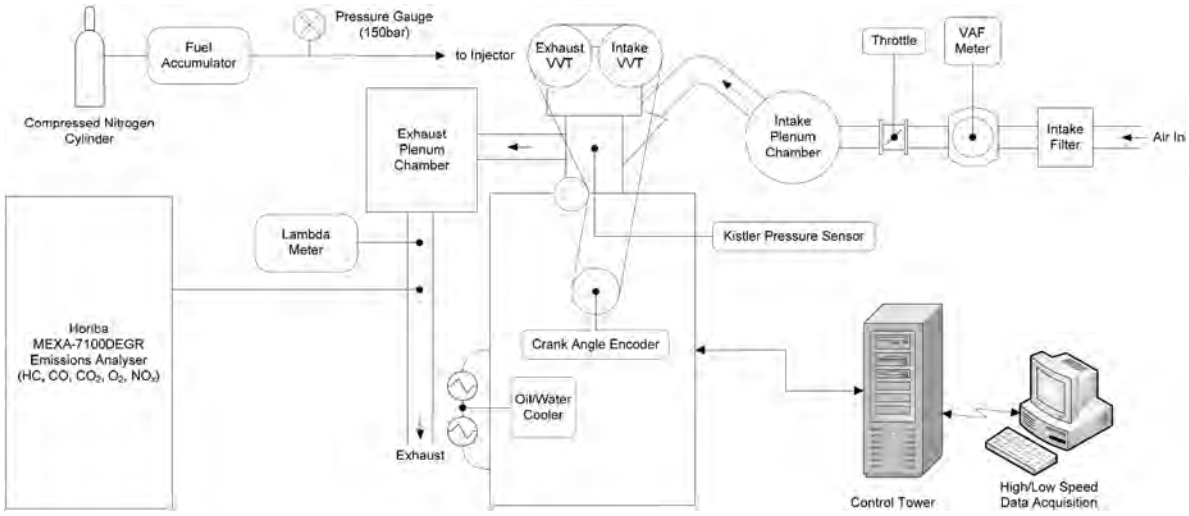

Figure 1. Schematic of engine and instrumentation setup

EMISSIONS AND FUEL MEASUREMENT

The gaseous emissions were quantified using a Horiba MEXA-7100DEGR gas tower. Exhaust samples were taken 0.3m downstream of the exhaust valve and were pumped via a heated line (maintained at 191°C) to the analyzer.

The fuel consumption was calculated using the volumetric air flow rate (measured by a positive displacement rotary flow meter) and the actual lambda value (Bosch heated LSU wideband lambda sensor and ETAS LA4 lambda meter). The LA4 lambda meter uses fuel-specific curves to interpret the actual AFR using the oxygen content in the exhaust. Before each test, the user inputs the fuel's hydrogen-to-carbon (H/C) and oxygen-to-carbon (O/C) ratios, as well as the stoichiometric AFR (AFR_{stoich}), so that the fuel composition can be used to characterize the fuel curves.

TEST FUELS

The DMF used in this study was supplied by Shijiazhuang Lida Chemical Co. Ltd, China at 99.8% purity. This was benchmarked against commercial 97RON gasoline and to ethanol, which were both supplied by Shell Global Solutions, UK. The high octane gasoline was chosen as this represents the most favorable characteristics offered by the market and provides a strong benchmark to the two biofuels. The fuel characteristics are shown in Table 1.

Table 1. Test Fuel Properties

	DMF	Ethanol	Gasoline
Chemical Formula	C_6H_8O	C_2H_6O	C_2-C_{14}
H/C Ratio	1.333	3	1.795
O/C Ratio	0.167	0.5	0
Gravimetric Oxygen Content (%)	16.67	34.78	0
Density @ 20ºC (kg/m^3)	889.7*	790.9*	744.6
Research Octane Number (RON)	101.3†	107‡	96.8
Motor Octane Number (MON)	88.1†	89‡	85.7
Octane Index, (K = 0.5)	94.7	98	91.25
Stoichiometric Air Fuel Ratio	10.72	8.95	14.46
LCV (MJ/kg)	32.9*	26.9*	42.9
LCV (MJ/L)	29.3*	21.3*	31.9
Flash Point (ºC)	1	13	-40
Heat of Vaporization (kJ/kg)	332	840‡	373
Initial Boiling Point (ºC)	92	78.4	32.8

**Measured at the University of Birmingham*
†API Research Project 45 (1956) and Phillips data.
‡Heywood, J.B., Internal Combustion Engine Fundamentals. 1988: McGraw-Hill [19]

EXPERIMENTAL PROCEDURE

The engine was considered warm once the coolant and lubricating oil temperatures had stabilized at 85±5°C and 95±3°C, respectively. All tests were carried out at a constant engine speed of 1500rpm and ambient air intake conditions (approximately 25±2°C). Sweeps were performed using each sensitivity parameter. During these sweeps the remaining

parameters were fixed at the reference engine operating conditions, as shown in Table 2. Here (regardless of the load), the engine is run at AFR_{stoich} (λ=1), 280°$bTDC_{comb}$ start of injection timing (SOI), 16°$bTDC_{intake}$ intake valve open (IVO) timing, 36°$aTDC_{intake}$ exhaust valve close (EVC) timing and MBT ignition timing. These MBT timings can be found in a previous publication [11]. The pressure data from 300 consecutive cycles was recorded for each test using the in-house developed LabVIEW code.

Table 2. Engine Specification

Engine Type	4-Stroke, 4-Valve
Combustion System	Spray-Guided DISI
Swept Volume	565.6cm^3
Bore x Stroke	90 x 88.9mm
Compression Ratio	11.5:1
Engine Speed	1500rpm
Injector	Multi-hole Nozzle
Fuel Pressure and Timing	150bar, 280º$bTDC_{comb}$
Intake Valve Opening	16º$bTDC_{intake}$
Exhaust Valve Closing	36º$aTDC_{intake}$

When changing fuels, the high pressure fuelling system was purged using nitrogen until the lines were considered clean. Once the supply line was re-pressurized to 150bar using the new fuel, the engine was run for several minutes. This removed any previous fuel from the injector tip and in any combustion chamber crevices before the data was acquired. The ETAS LA4 lambda meter settings were changed for each fuel using the AFR_{stoich}, O/C and H/C ratios in Table 2.

PARAMETER SWEEPS

Sweeps of each of the four key engine parameters were performed, whilst maintaining the other variables at the reference engine condition shown in Table 2. Each of the sweeps were generated between 3.5bar and 8.5bar IMEP (low and high engine loads, respectively), in 1bar IMEP intervals and at a fixed engine speed of 1500rpm. During each sweep, the throttle and ignition timings (except for the ignition timing sweeps) remained constant (generated at the reference condition). This was used in order to increase repeatability. The method for performing each sweep is discussed in turn.

Firstly, ignition timing sweeps were performed to analyze the sensitivity of IMEP when retarding, or advancing (where possible) from the optimum timing at the reference condition. As used in other studies by the authors and commonly employed by other researchers, the MBT, or optimum ignition timing is defined as the ignition timing to produce the maximum IMEP for a fixed throttle position. If audible knock occurred, the MBT timing was retarded by 2CAD, an arbitrarily safe margin, as advised by key engine researchers [19, 33]. Retarding the timing further for emissions preservation was not used, in order to eliminate subjectivity and better isolate the effect of ignition timing sensitivity. At each load, the ignition timing was advanced to find the knock limit or until a significant drop in performance or stability was seen (IMEP decrease from MBT > 5% or COV of IMEP increase from MBT > 3%). Similarly, the ignition timing was retarded until this aforementioned drop in performance was also seen. At each load the throttle was kept constant so that the drop in performance and emissions would be easily repeatable and the fuel injection pulse-width was adjusted finely (±1μs) to find stoichiometry.

Secondly, SOI timing sweeps were conducted either side of 270°$bTDC_{comb}$. Although this is not the reference SOI timing condition, when using intervals of 30CAD, the behavior at TDC and BDC was neatly included. Firstly, the SOI timing was advanced to 360°$bTDC_{comb}$ (TDC) and then retarded to 180°$bTDC_{comb}$ (BDC) with two records of 270°$bTDC_{comb}$ in the process. This allows the effect of any engine drift during the sweeps to be observed and accounted for.

Thirdly, AFR sweeps were determined using the injector pulse-width, once the desired load was found at stoichiometry. Firstly, the AFR was made increasingly rich (λ<1) until λ=0.8 was reached and then lean until the lean limit was reached; determined by high combustion instability, or when the COV of IMEP exceeded 5%. The results at stoichiometry (λ=1) were recorded before each rich and lean sweep.

Finally, the IVO and EVC timings were varied either side of their respective middle points (0°aTDC, IVO and 20°aTDC, EVC) in 5CAD intervals with a 40CAD range. Once again, this middle point was recorded twice.

For each set of tests, several repeats were made with each fuel to produce an average and error bars have been shown in the graphs where applicable in order to highlight such variations.

RESULTS AND DISCUSSION

The results from the various sweeps are shown in the following section. The most interesting relationships are discussed in order to better understand and quantify the sensitivity to each parameter.

COMBUSTION PHASING

The effect of ignition timing has a direct effect on the combustion phasing. Therefore the variation of engine load (IMEP) due to the sensitivity of ignition timing is examined in order to quantify differences between the three fuels.

The variation of IMEP using DMF, ethanol and gasoline at the highest load ignition timing sweep (approximately 8.5bar IMEP) is shown in Figure 2a. At this load, there is a clear difference between the three fuels. Ethanol combustion, which is uninhibited by knock at this compression ratio (11.5:1), permits a wide ignition timing sweep and allows the IMEP to be analyzed either side of the MBT timing (21°bTDC). DMF and gasoline on the other hand, are much

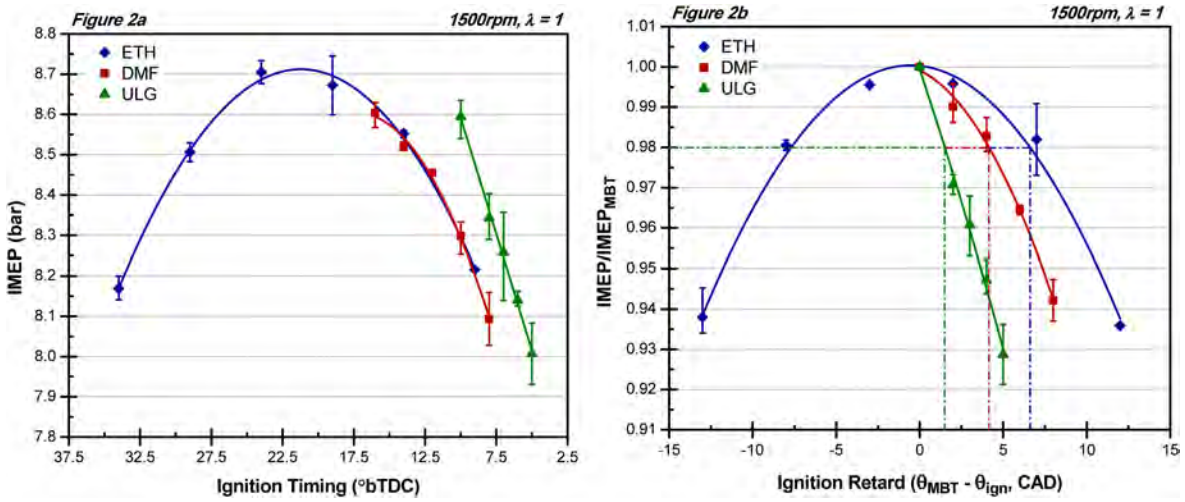

Figure 2. Ignition Timing: Effect of ignition timing on IMEP (a) and ignition retard on normalized IMEP (b) at high load when using ethanol, DMF and gasoline

more sensitive to the onset of knock and only the retarded timing from MBT can be observed. With comparison, there appears to be a relationship between the MBT location and rate of change of IMEP; the more retarded the MBT timing is, the higher the rate of IMEP decay becomes with ignition retard. This rate of decay can be used as an indicator of the ignition timing sensitivity for each fuel.

When normalizing the IMEP and ignition timing data (by their respective MBT timings) from Figure 2a, these fuel effects become more obvious. This is shown in Figure 2b, using the term ignition retard, which represents the number of retarded CAD from MBT. As the term suggests, a positive value represents retarded timing from MBT, whereas a negative value is advanced. This approach was previously used by Ayala et al. [34] to help develop their combustion retard parameter.

When using ethanol, the rate of decay is symmetrical about its MBT timing and decreases at a lower rate than with DMF and gasoline. This is largely explained by the knock suppression superiority of ethanol. Clearly, within this range of IMEP decay, ethanol is the least sensitive to ignition timing variations. Typically, once the MBT timing is found, engine developers employ an ignition retard for emissions preservation. This is commonly the ignition retard that produces an IMEP of 2% less than that from MBT. Therefore, dashed lines have been used in Figure 2b to highlight the variation of permitted ignition retard between the three fuels, and hence help quantify ignition timing sensitivity. The near equal separation between the three fuels mirrors the near equal separation in anti-knock, or octane index (OI), shown in Table 1. This effect becomes clearer when examining all loads, as shown in Figure 3.

Figure 3 presents the permissible ignition retard for a 2% drop in IMEP from MBT at all loads for gasoline, ethanol and DMF; the greater the permissible ignition retard, the wider the ignition timing window (greater opportunity for emissions optimization). Each result is interpolated using the ignition timing sweeps. For all fuels, the ignition timing window is the widest at the lowest load and generally decreases with increasing in load. The low ignition timing sensitivity of ethanol is consistent with load and generates a gap of approximately 5CAD with gasoline from loads of 5.5bar IMEP and above. DMF resides between gasoline and ethanol from this point.

The benefits of widened ignition timing windows are shown in Figure 3b. Here, the effect of ignition retard on indicated specific NO_x ($isNO_x$) emissions is shown for all loads. It is clear that the $isNO_x$ reduction is more effective with ethanol than with gasoline and DMF. At low load (3.5bar IMEP) this reduction with ethanol is as high as 64% and steadily decreases with load to 25% at 8.5bar IMEP. With DMF, the $isNO_x$ reduction is consistently similar to gasoline despite the greater ignition timing window. Between 3.5bar and 8.5bar IMEP, the reduction is 37% and 8%. In previous work by the authors, DMF has been shown to produce higher $isNO_x$ emissions than both ethanol and gasoline possibly due to the higher peak combustion temperatures or residency times, which might explain the low decrease with high ignition retard [11].

INJECTION TIMING

The advent of DI has introduced a new engine control variable; the SOI timing. This influences the volumetric efficiency (VE) and ultimately affects the performance. The varying extent of charge-cooling on engine performance is examined to show the sensitivities between each fuel.

The effect of varying the SOI timing on VE and IMEP using the three fuels is shown in Figure 4a and Figure 4b, respectively. The data from the highest load (8.5bar IMEP) is shown as this presents the greatest differences between the fuels. As previously discussed, the injection window of

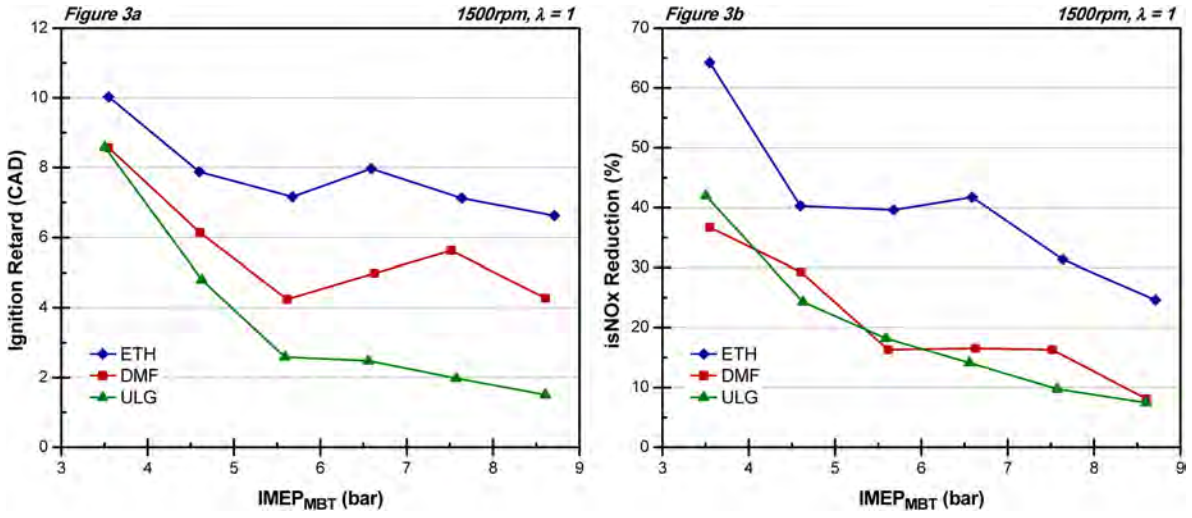

Figure 3. <u>Ignition Timing:</u> Ignition retard to obtain 2% decrease in maximum IMEP from MBT (a) and the effect of this ignition retard on normalized indicated specific nitrogen oxide (isNO$_x$) emissions (b) at all engine loads when using ethanol, DMF and gasoline

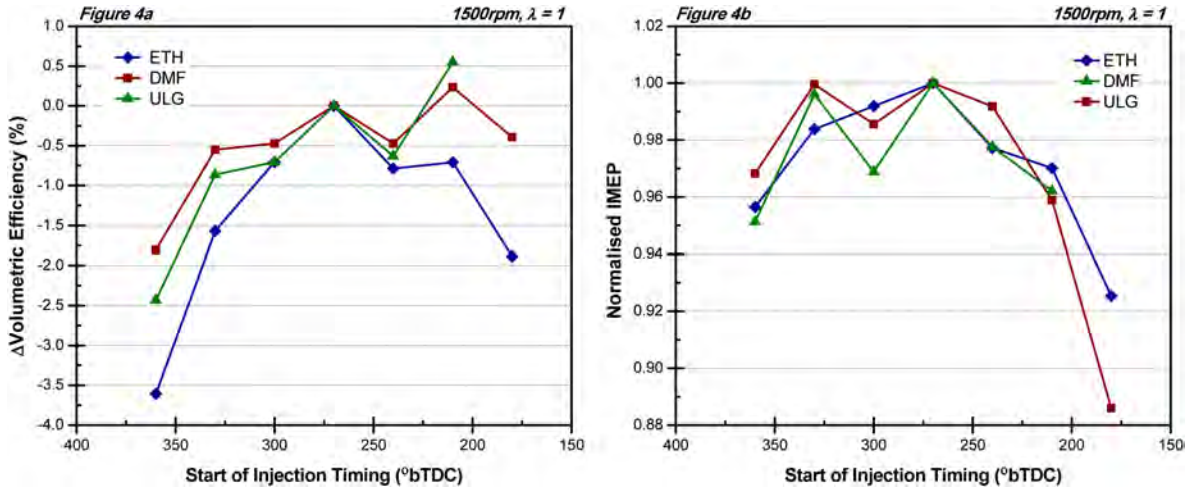

Figure 4. <u>SOI Timing:</u> Change in VE (a) and IMEP (b) at high load with varying SOI timing from 270°bTDC$_{comb}$ when using ethanol, DMF and gasoline

360-180°bTDC$_{comb}$ (in 30CAD increments) was chosen in order to highlight the positive impact of charge-cooling during the intake stroke (IVO/IVC = 376/126°bTDC$_{comb}$. The record of SOI timings at 30CAD intervals allows the inclusion of TDC, BDC and mid-way through the stoke when the piston speed is close to its greatest, as used by Yang and Anderson [35]. As shown using ethanol in Figure 4a, the peak volumetric efficiency actually occurs near to the point of maximum piston speed (270°bTDC$_{comb}$). This increase is due to the spray 'chasing' the piston, which minimizes fuel impingement on the piston crown and increases intake charge density. The loss of VE (and reduced IMEP) with early SOI timing (360°bTDC$_{comb}$) is believed to be attributed to the high penetration rate causing piston impingement and loss of cooling [36]. With later SOI timings, the VE for ethanol decays. This is because the intake air flow rate reduces and decreases the amount of heat transfer during charge-cooling. However, when the SOI timing is 210°bTDC$_{comb}$, the VE for the three fuels increases (although less for ethanol). It is probable that at this point, the interaction between the air flow and the fuel spray is increased due to changes in turbulence and to the flow distribution.

In terms of emissions, the SOI timing has a significant impact. Early SOI timings improve the homogeneity of the mixture but might result in piston impingement. Later SOI timings reduce the homogeneity but avoid such piston wetting. Furthermore, the effect on charge temperature varies the initial conditions; if the cooling occurs too soon the

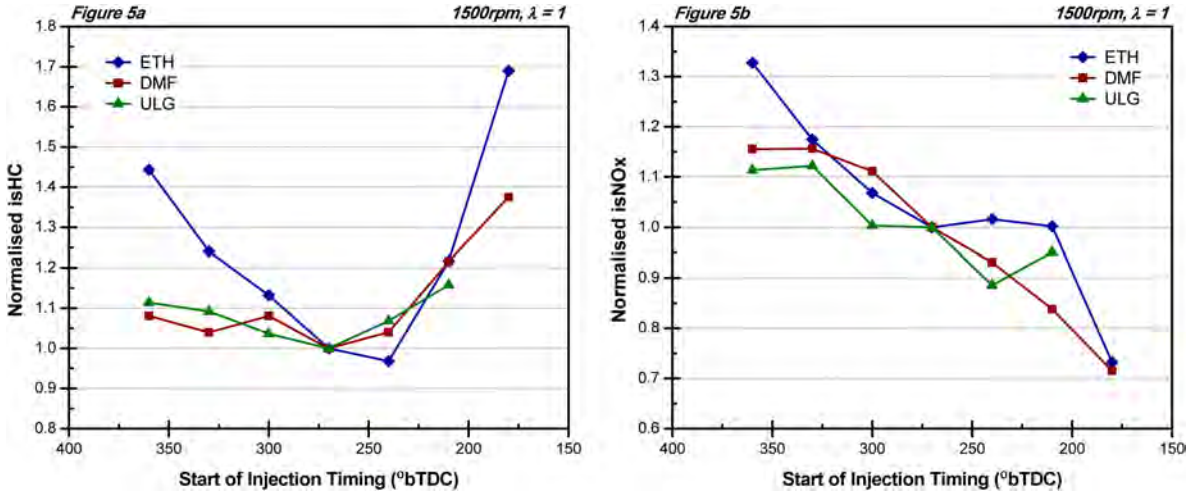

Figure 5. SOI Timing: Normalized isHC (a) and isNO$_x$ (b) emissions at high load with varying SOI timing from at 270°bTDC$_{comb}$ when using ethanol, DMF and gasoline

temperature at the point of ignition will be higher than later injections and would result in more NO_x emissions. The effect of SOI timing variations on unburned hydrocarbons is shown in Figure 5a. For gasoline and DMF, the lowest indicated specific hydrocarbons (isHCs) are emitted at 270°bTDC$_{comb}$. For ethanol, the lowest isHC is found at the latest point in the SOI timing window (2% decrease in IMEP) around 240°bTDC$_{comb}$. Clearly, there are trade-offs when finding the optimum SOI timing. In terms of isNO_x emissions, the later the timing, the greater the reduction. When using gasoline and DMF, the isNO_x emissions can be reduced by 10% at the latest acceptable SOI timings. When using ethanol, on the other hand, there is no effect on isNO_x emissions within the SOI timing window. In summary, each fuel does have varying sensitivities to SOI timing and, in general, the widest window for optimization is found with the fuels with the lowest heat of vaporization.

RELATIVE AIR-FUEL RATIO

Most modern engines are calibrated to run under stratified conditions. This allows the losses due to throttling to be reduced or even eliminated and helps to increase the fuel conversion efficiency. This also helps to dramatically reduce CO and NO_x emissions as the combustion efficiency is increased. However, as the mixture becomes leaner, the combustion stability decreases. As the AFR sweeps used in this study use fixed throttle and ignition timing and not the same IMEP (only at λ=1), the IMEP is greatly reduced at the lean limit. Therefore, instead of using the 2% drop in IMEP as a marker to sensitivity, the AFR window is governed by the upper combustion stability limit of 5% COV of IMEP.

The AFR sweeps for the three fuels at 8.5bar are shown in Figure 6a. Clearly, the differences between the fuels are apparent at this high load. Here, both biofuels show lower sensitivities to changes in AFR than with gasoline. This has been seen in previous work by the authors [11] and is because single component oxygenated fuels burn more rapidly [37]. Ethanol has a higher concentration of oxygen and lower number of molecule when compared to DMF (see Table 1). This helps the combustion of ethanol to produce the lowest combustion instabilities and thus widen the AFR window. When using gasoline, which has no oxygen content and a mixture of short and long chain HCs, the COV of IMEP rises quickly above 3% when rich ($\lambda \geq 0.95$). For DMF and ethanol, this instability is reached as the mixture is leaned and is much less sensitive.

Figure 6b shows the effect on indicated efficiency as the mixture is leaned and is normalized about the stoichiometric condition. Here, the indicated efficiency at the lean limit is on the declining slope of the maximum indicated efficiency. For gasoline, the maximum is around $\lambda = 1.1$, whereas the lean limit is at $\lambda = 1.24$. Within this AFR range the indicated efficiency drops by 1.7%. However, for DMF and ethanol, the effect on indicated efficiency around their respective lean limits is minimal (when using DMF, the indicated efficiency actually increases by 0.3%). Therefore, as the lean limit increases, the sensitivity of the indicated efficiency reduces, which reduces the proximity to the maximum indicated efficiency.

When analyzing the lean limit for all three fuels at every initial load, the difference in sensitivity becomes clear. In some cases, when the AFR at 5% COV of IMEP was not directly recorded, the trend has been interpolated using surrounding values. However, as with ethanol at 8.5bar IMEP (see Figure 6a), some points required extrapolation. Nevertheless, the lowest COV of IMEP which required extrapolation was 4.5%. In Figure 7a, the lean limit with ethanol is consistently higher than with DMF and gasoline, which increases with load for all three fuels. When the load increases above 6.5bar IMEP, the difference in the lean limit between DMF and ethanol begins to increase.

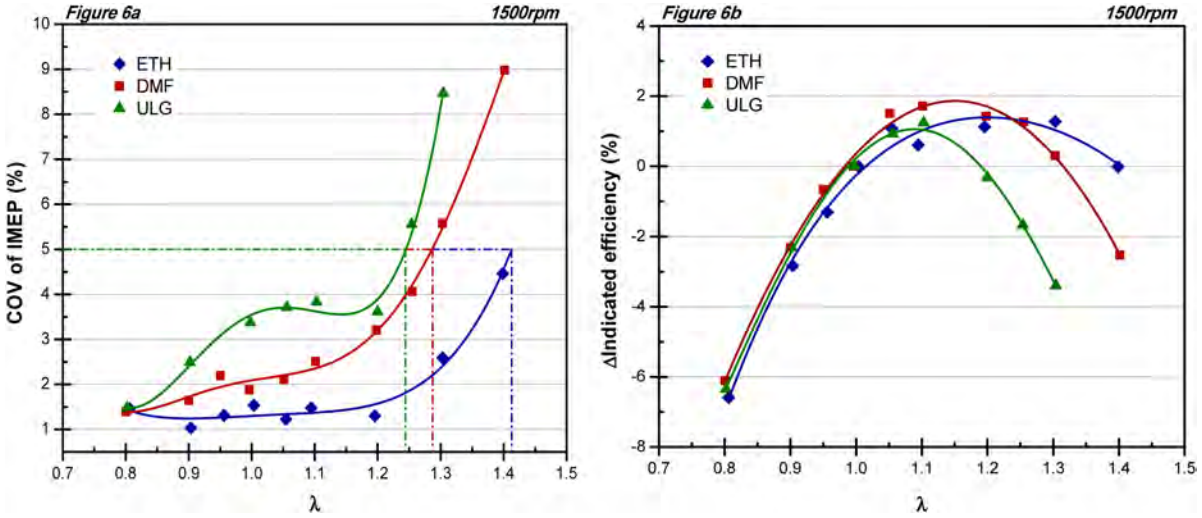

Figure 6. AFR: Change in COV of IMEP at high load (a) and indicated efficiency (b) with varying AFR when using ethanol, DMF and gasoline

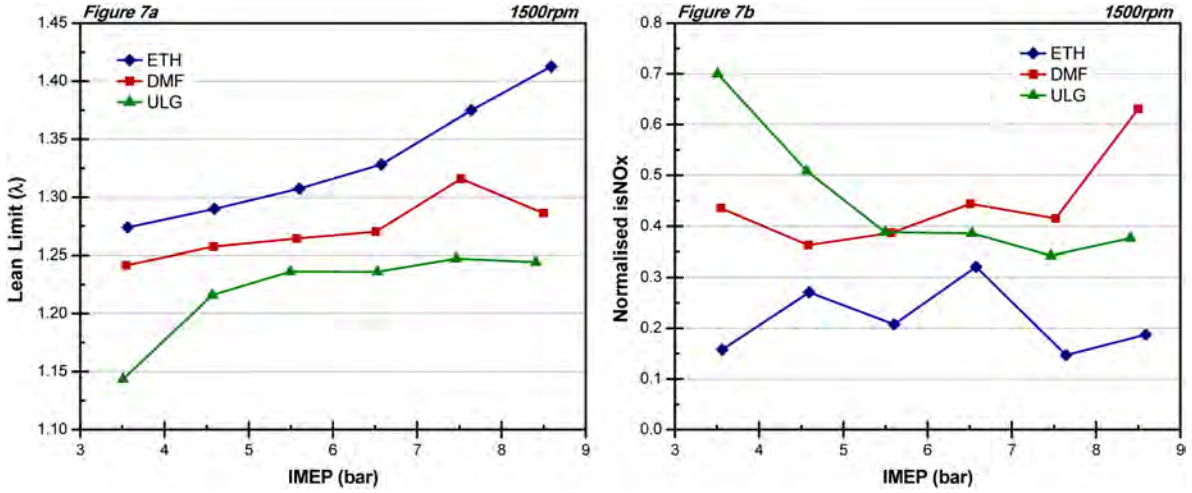

Figure 7. AFR: Lean limit (a) and normalized isNO$_x$ (b) at each load when using ethanol, DMF and gasoline

The benefits of the lean limit also become apparent when analyzing the isNO$_x$ emissions, as shown in Figure 7b. Here, the isNO$_x$ emissions are greatly reduced when using ethanol at the lean limit consistently with load. Below 5.5bar IMEP, DMF produces greater decreases in isNO$_x$ than with gasoline but is superseded by gasoline at higher loads. Clearly, the reduced ability to reduce NO$_x$ emissions when using DMF is an area of concern. This is possibly due to the higher combustion temperatures when using DMF which might be overcome by the use of exhaust gas recirculation (EGR).

INTAKE VALVE TIMING

Most advanced modern engines are equipped with variable valve timing systems. By varying the IVO timing, the charge air flow can be optimized at the various engine speeds and loads in a typical duty cycle. The analysis focuses on the effect of IVO timing at high load (8.5bar IMEP) because the trend is magnified.

The IVO timing directly influences the VE, as shown in Figure 8a. Here, the change in VE either side of the maximum shows a clear separation between the three fuels. At the 2% drop in VE, gasoline presents the narrowest window of IVO variation, whereas ethanol and DMF produce a wider window in which to optimize for efficiency. Between DMF and ethanol, there is little separation in terms of change in VE although ethanol is marginally less sensitive. The effect of VE on IMEP is shown in Figure 8b. Here, the maximum IMEP coincides with the maximum VE. At the edge of the sweep, with the most advanced IVO timing, the IMEP, when using gasoline drops by 24% from the IVO at maximum VE. For DMF and ethanol this decrease is 20% and 16% respectively, as the sensitivity is lower.

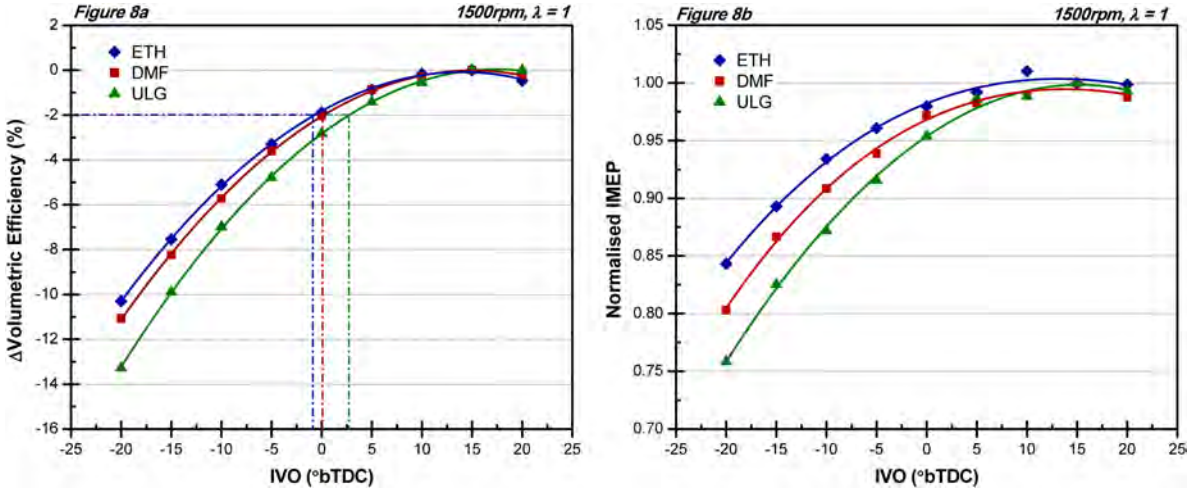

Figure 8. Intake Valve Timing: Change in VE (a) and normalized IMEP (b) at high load with varying IVO timing from 15°bTDC$_{intake}$ when using ethanol, DMF and gasoline

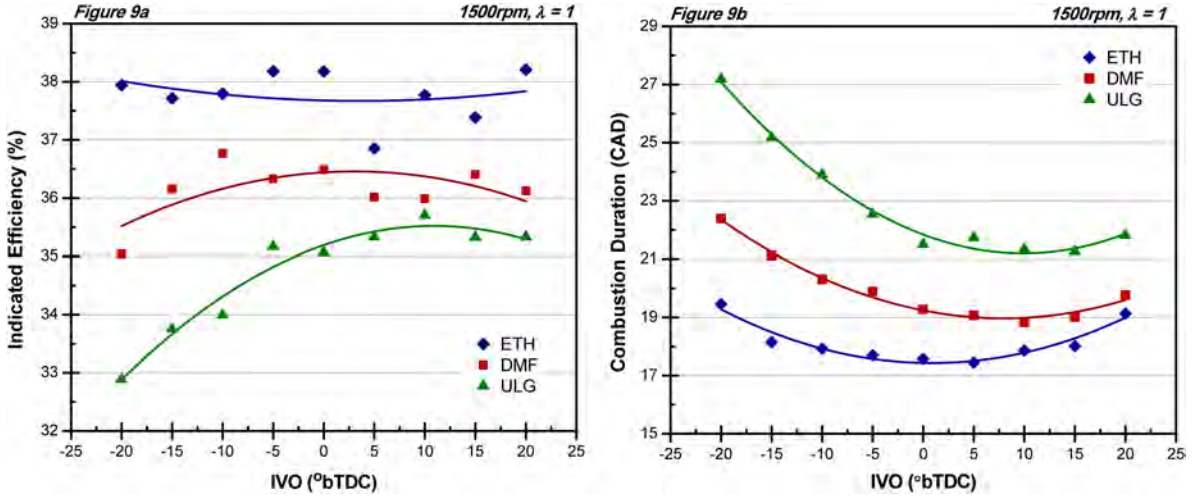

Figure 9. Intake Valve Timing: Indicated efficiencies (a) and combustion durations (b) at high load with varying IVO timing when using ethanol, DMF and gasoline

When examining the effect on indicated efficiency, as shown in Figure 9a, the benefits of the wider IVO window are more apparent. This is because, the maximum indicated efficiency is found marginally later than the maximum IMEP or VE. This valve timing location is also related to the sensitivity and retards as the sensitivity reduces. For gasoline and DMF, the maximum indicated efficiencies (based on the line of best fit) are obtained because these points are within the IVO windows. For ethanol, the indicated efficiency is almost constant throughout the entire range. The location of maximum indicated efficiency is determined by the location of the lowest combustion duration, as shown in Figure 9b. Here, ethanol shows little variation but with a clear minimum combustion duration with IVO timing at TDC. For DMF and gasoline the minimum combustion duration is increasingly more advanced.

EXHAUST VALVE TIMING

The EVC timing is also a modern engine control parameter and helps to control the internal trapped residuals, which have a direct impact on the emissions rather than performance. In this analysis, the sensitivity of each fuel to EVC timing is quantified at the 2% drop in IMEP. From this point, the extent of emissions reduction is then examined.

The effect of varying the EVC timing on IMEP is shown in Figure 10a. Here, because the maximum IMEP is found towards the middle of the sweep, the 2% drop in IMEP encloses a wide range of EVC timings. As with the previous engine parameters, ethanol generates the widest EVC timing window and gasoline generates the least (shown by the dashed lines). The window for ethanol is 9.5CAD more than with DMF, which, in turn, is 4CAD more than with gasoline.

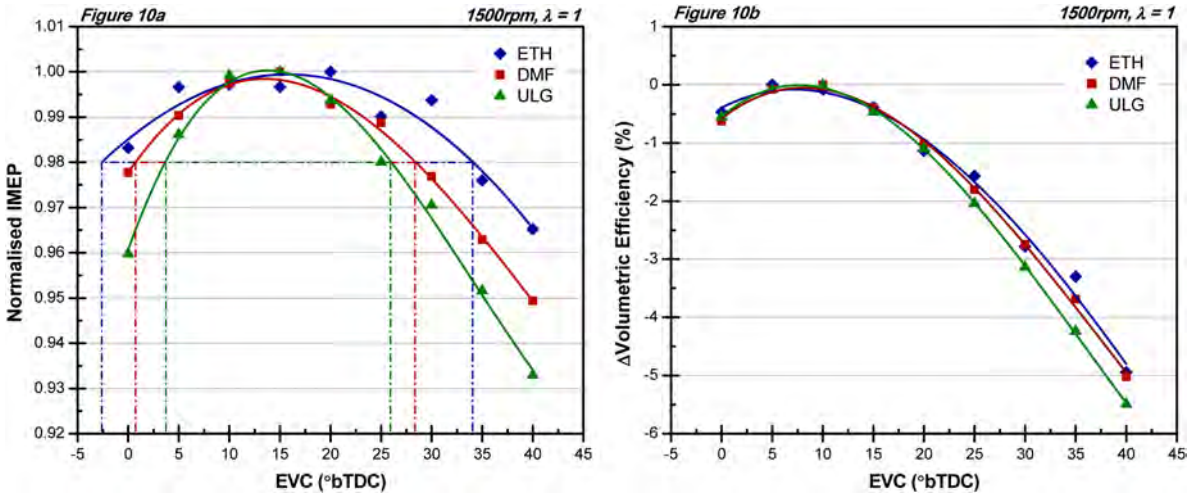

Figure 10. Exhaust Valve Timing: Change in normalized IMEP (a) and VE (a) at high load with varying EVC timing when using ethanol, DMF and gasoline

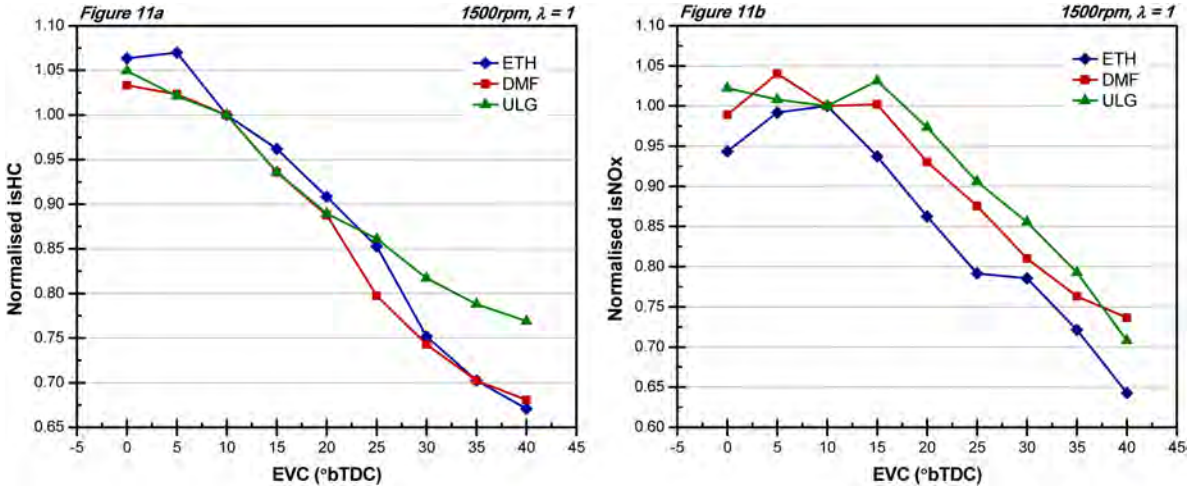

Figure 11. Exhaust Valve Timing: Change in normalized isHC (a) and isNO$_x$ (b) at high load with varying EVC timing when using ethanol, DMF and gasoline

At the latest EVC timing, the IMEP with ethanol is only reduced by 3.5%. However, with gasoline this reduction is almost double. Nevertheless, the separation between the fuels with VE is less evident, as shown in Figure 10b.

The effect of EVC timing on isHC and isNO$_x$ emissions is shown in Figure 11a and Figure 11b, respectively. Clearly, as the EVC timing is retarded, the emissions are reduced. The most retarded EVC timings within the permissible EVC range (2% IMEP drop) for DMF and ethanol allow an approximate 25% and 30% reduction in isHC emissions, respectively. For gasoline however, because the sensitivity to EVC timing is higher, the maximum reduction in isHC is only 15%. This trend is magnified with isNO$_x$ emissions because the fuels also have a varying sensitivity to EVC timing. For the three fuels, the isNO$_x$ emissions reductions increase in the order of gasoline, DMF and then ethanol with reductions of approximately 10%, 18% and 28%, respectively. Clearly, the biggest reductions are found with ethanol, which benefit from reduced sensitivity to IMEP as well as individual emissions.

CONCLUSIONS

This study compares the sensitivity of DMF (2,5-dimethylfuran) to commercial gasoline and ethanol, using four engine control parameters: ignition timing, injection timing, AFR, and valve (intake and exhaust) timing. The engine tests were performed using sweeps of the various control parameters on a single cylinder DISI engine from 3.5bar to 8.5bar IMEP in 1bar IMEP increments and at a fixed engine speed of 1500rpm. Only the most significant behavior is analyzed and gives a good overview of the varying fuel sensitivity. Based on these experiments, the following conclusions can be drawn:

i. The three fuels tested have varying sensitivities to the combustion parameters tested. With the exception of injection timing, the order of sensitivity was: gasoline > DMF > ethanol.

ii. Ignition Timing: The sensitivity to ignition timing was linked to the octane number of each fuel. The sensitivity when using DMF was lower than that with gasoline (due to the higher octane number). At 8.5bar IMEP, the ignition retard to maintain a 2% decrease in peak IMEP was 4.3CAD with DMF, compared to 1.5 CAD and 6.6CAD with gasoline and ethanol, respectively. This increased ignition retard allows isNO_x reductions of up to 37% (at 3.5bar IMEP) to be found with DMF. Such reductions are consistent to gasoline with load. However, the lower ignition timing sensitivity of ethanol consistently produces the highest reductions in isNO_x emissions (up to 64% at 3.5bar IMEP).

iii. SOI Timing: With injection timing variations, DMF showed the lowest sensitivity to VE, whereas ethanol showed the highest sensitivity due to the greater effect of charge-cooling. This allows a wider window for emissions optimization when using DMF. At 8.5bar IMEP, the SOI timing window to produce a 2% drop in IMEP (from the maximum) was 120CAD with DMF, compared to 90CAD with ethanol. The latest SOI timings (within this window) produced the lowest isNO_x emissions with DMF, up to 10% (similar to gasoline).

iv. AFR: In terms of AFR, the sensitivity when using DMF was lower than with gasoline but higher than with ethanol. At 8.5bar IMEP, the limit of lean combustion (COV of IMEP $\leq$ 5%) for DMF was λ=1.29, whereas for gasoline this was λ=1.24 (λ=1.41 for ethanol). At this point, the indicated efficiency for gasoline decreases by 1.7% but there is minimal change for DMF and ethanol (the indicated efficiency actually increases by 0.3% when using DMF). However, the isNO_x emissions reductions were lower for DMF (37%) than for gasoline (62%) an ethanol (81%) at this 8.5bar IMEP.

v. Valve Timing: The reduced sensitivity of DMF to both intake and exhaust valve timing (compared to gasoline) helps to maintain high indicated efficiency and isHC and isNO_x emissions reduction. For instance, the earliest EVC timing permitted within the 2% drop in IMEP at 8.5bar IMEP produces reductions in isHC and isNO_x when using DMF of 25% and 12.5%, respectively. For gasoline this equates to 15% (isHC) and 10% (isNO_x).

In summary, these experiments highlight the reduced sensitivity of key engine control parameters (ignition timing, injection timing, AFR and valve timing) when using DMF and ethanol over commercial gasoline. This is largely due to the greater resistance of these fuels to engine knock but is also affected by the cooling effect. Reduced sensitivities allow a wider window for efficiency and emissions optimization.

ACKNOWLEDGMENTS

The present work is part of a 3-year research project sponsored by the Engineering and Physical Sciences Research Council (EPSRC) under the grant EP/F061692/1. The authors would like to acknowledge the support from Jaguar Cars Ltd, Shell Global Solutions and various research assistants and technicians. The authors are also grateful for the financial support from the European Regional Development Fund (EUDF) and Advantage West Midlands (AWM). Finally, the authors would like to acknowledge the support from their international collaborators at Tsinghua University, China.

REFERENCES

1. Roman-Leshkov, R., Barrett, C.J., Liu, Z.Y. and Dumesic, J.A., *Production of Dimethylfuran for Liquid Fuels from Biomass-Derived Carbohydrates*. Nature, 2007. 447: p.982-986.
2. Dumesic, J.A., Roman-Leshkov, Y. and Chheda, J.N., *Catalytic Process for Producing Furan Derivatives from Carbohydrates in a Biphasic Reactor*. WO 2007/146636. World Intellectual Property. 2007: US.
3. Chidambaram, M. and Bell, A.T., *A Two-Step Approach for the Catalytic Conversion of Glucose to 2,5-Dimethylfuran in Ionic Liquids*. The Royal Society of Chemistry, 2010. 12: p.1253-1262.
4. Mascal, M. and Nikitin, E.B., *Direct, High-Yield Conversion of Cellulose into Biofuel*. Angewandte Chemie Internation Edition, 2008. 47: p.7924-7926.
5. Thananatthanachon, T. and Rauchfuss, T. B., *Efficient Production of the Liquid Fuel 2,5-Dimethylfuran from Fructose Using Formic Acid as a Reagent*. Angewandte Chemie Internation Edition, 2010. 49: p. 6616-6618.
6. Yang, F., Liu, Q., Bai, X. and Du, Y., *Conversion of Biomass into 5-Hydroxymethylfurfural using Solid Acid Catalyst*. Bioresource Technology, 2011. 102: p.3424-3429.
7. Zhao, H., Holladay, J.E., Brown, H. and Zhang, Z.C., *Metal Chlorides in Ionic Liquid Solvents Convert Sugars to 5-Hydroxymethylfurfural*. Science, 2007. 316: p.1597-1600.
8. Luque, R., Herrero-Davila, L., Campelo, J.M., Clark, J.H, Hidalgo, J.M., Luna, D., Marinasa, J.M. and Romeroa, A.A., *Biofuels: a Technological Perspective*. Energy and Environmental Science, 2008. 1(5): p.513-593.
9. Zhong, S., Daniel, R., Xu, H., Zhang, J., Turner, D., Wyszynski, M.L. and Richards, P., *Combustion and Emissions of 2,5-Dimethylfuran in a Direct-Injection Spark-Ignition Engine*. Energy and Fuels, 2010. 24(5): p.2891-2899.
10. Wu, X., Daniel, R., Tian, G., Xu, H., Huang, Z. and Richardson, D., *Dual-injection: The flexible, Bi-Fuel Concept for Spark-Ignition Engines Fuelled with Various Gasoline and Biofuel Blends*. Applied Energy, 2011. 88: p.2305-2314.
11. Daniel, R., Tian, G., Xu, H., Wyszynski, M.L., Wu, X. and Huang, Z., *Effect of Spark Timing and Load on a DISI Engine Fuelled with 2,5-Dimethylfuran*. Fuel, 2011. 90: p.449-458.
12. Wu, X., Huang, Z., Jin, C., Wang, X., Zheng, B., Zhang, Y. and Wei, L., *Measurements of Laminar Burning Velocities and Markstein Lengths of 2,5-Dimethylfuran-Air-Diluent Premixed Flames*. Energy and Fuels, 2009. 23: p.4355-4362.
13. Wu, X., Huang, Z., Jin, C., Wang, X. and Wei, L., *Laminar Burning Velocities and Markstein Lengths of 2,5-Dimethylfuran-Air Premixed Flames at Elevated Temperatures*. Combustion Science and Technology, 2011. 158: p.220-237.
14. Wu, X., Huang, Z., Wang, X., Jin, C., Tang, C., Wei, L., Law, C.K., *Laminar Burning Velocities and Flame Instabilities of 2,5-Dimethylfuran-Air Mixtures at Elevated Pressures*. Combustion and Flame, 2011. 158: p.539-546.
15. Tian, G., Daniel, R., Li, H., Xu, H., Shuai, S. and Richards, P., *Laminar Burning Velocities of 2,5-Dimethylfuran compared with Ethanol and Gasoline*. Energy and Fuels, 2010. 27(7): p.3898-3905.
16. Tian, G., Li, H., Xu, H., Li, Y. et al., "Spray Characteristics Study of DMF Using Phase Doppler Particle Analyzer," *SAE Int. J. Passeng. Cars - Mech. Syst.* 3(1):948-958, 2010, doi:10.4271/2010-01-1505.
17. Wu, X., Huang, Z., Yuan, T., Zhang, K. and Wei, L., *Identification of Combustion Intermediates in a Low-Pressure Premixed Laminar 2,5-Dimethylfuran/Oxygen/Argon Flame with Tunable Synchrotron Photoionization*. Combustion and Flame, 2009. 156: p.1365-1376.
18. Tian, G., Daniel, R. and Xu, H., *DMF - a New Biofuel Candidate*, Biofuel Production - Recent Developments and Prospects. 2011, InTech.

19. Heywood, J.B., *Internal Combustion Engine Fundamentals*. 1988: McGraw-Hill.
20. Roepke, K., Rosenek, A., and Fischer, M., "Practical application of DoE methods in the development of production internal combustion engines," SAE Technical Paper 2002-04-0083, 2002.
21. Stuhler, H., Kruse, T., Stuber, A., Gschweitl, K. et al., "Automated Model-Based GDI Engine Calibration Adaptive Online DoE Approach," SAE Technical Paper 2002-01-0708, 2002, doi:10.4271/2002-01-0708.
22. Guerrier, M. and Cawsey, P., "The Development of Model Based Methodologies for Gasoline IC Engine Calibration," SAE Technical Paper 2004-01-1466, 2004, doi:10.4271/2004-01-1466.
23. Alkidas, A. and El Tahry, S., "Contributors to the Fuel Economy Advantage of DISI Engines Over PFI Engines," SAE Technical Paper 2003-01-3101, 2003, doi:10.4271/2003-01-3101.
24. Zhao, F., Harrington, D.L. and Lai, M-C.D., "Automotive Gasoline Direct-Injection Engines," Society of Automotive Engineers, Inc., Warrendale, PA, ISBN: 978-0-7680-0882-1, 2002, doi:10.4271/R-315.
25. Hennessey, R., Fuentes, A., and Wicker, R., "Effect of Injection Timing on Piston Surface Fuel Impingement and Vaporization in Direct Injection, Spark Ignition Engines," SAE Technical Paper 2001-01-2025, 2001, doi:10.4271/2001-01-2025.
26. Chen, L., Braisher, M., Crossley, A., Stone, R. et al., "The Influence of Ethanol Blends on Particulate Matter Emissions from Gasoline Direct Injection Engines," SAE Technical Paper 2010-01-0793, 2010, doi: 10.4271/2010-01-0793.
27. Kapus, P., Fuerhapter, A., Fuchs, H., and Fraidl, G., "Ethanol Direct Injection on Turbocharged SI Engines - Potential and Challenges," SAE Technical Paper 2007-01-1408, 2007, doi:10.4271/2007-01-1408.
28. Dunn-Rankin, D., *Lean Combustion: Fundamentals, Applications, and Prospects*, Combustion Treatise Series, Elsevier, Editor. 2007.
29. Shayler, P., Jones, S., Horn, G., and Eade, D., "Characterisation of DISI Emissions and Fuel Economy in Homogeneous and Stratified Charge Modes of Operation," SAE Technical Paper 2001-01-3671, 2001, doi: 10.4271/2001-01-3671.
30. Iwachido, K., Onodera, T., Watanabe, T., Koyama, M. et al., "NOx Trap Catalyst Technologies to Attain 99.5% NOx Reduction Efficiency for Lean Burn Gasoline Engine Application," SAE Technical Paper 2009-01-1077, 2009, doi:10.4271/2009-01-1077.
31. Shayler, P., Jones, S., Horn, G., and Eade, D., "DISI Engine Spark and Fuel Injection Timings. Effects, Compromise and Robustness," SAE Technical Paper 2001-01-3672, 2001, doi:10.4271/2001-01-3672.
32. Sandford, M., Page, G., and Crawford, P., "The All New AJV8," SAE Technical Paper 2009-01-1060, 2009, doi:10.4271/2009-01-1060.
33. Stone, R., *Introduction to Internal Combustion Engines*. Third Edition. 1999: Macmillan Press Ltd.
34. Ayala, F., Gerty, M., and Heywood, J., "Effects of Combustion Phasing, Relative Air-fuel Ratio, Compression Ratio, and Load on SI Engine Efficiency," SAE Technical Paper 2006-01-0229, 2006, doi: 10.4271/2006-01-0229.
35. Yang, J. and Anderson, R., "Fuel Injection Strategies to Increase Full-Load Torque Output of a Direct-Injection SI Engine," SAE Technical Paper 980495, 1998, doi: 10.4271/980495.
36. Fry, M., King, J., and White, C., "A Comparison of Gasoline Direct Injection Systems and Discussion of Development Techniques," SAE Technical Paper 1999-01-0171, 1999, doi:10.4271/1999-01-0171.
37. de Francqueville, L., "Effects of Ethanol Addition in RON 95 Gasoline on GDI Stratified Combustion," SAE Technical Paper 2011-24-0055, 2011, doi:10.4271/2011-24-0055.

CONTACT INFORMATION

Professor Hongming Xu
School of Mechanical Engineering
University of Birmingham, Edgbaston
United Kingdom, B15 2TT
Tel: +44 (0)121 414 4153
h.m.xu@bham.ac.uk

DEFINITIONS

aTDC
After Top Dead Centre
bTDC
Before Top Dead Centre
CAD
Crank Angle Degrees
CO
Carbon Monoxide
CO_2
Carbon Dioxide
COV
Coefficient of Variation
DI
Direct-Injection
DISI
Direct-Injection Spark-Ignition
DMF
2,5-Dimethylfuran
ETH
Ethanol
EVC
Exhaust Valve Closure
HC
Hydrocarbon
IMEP
Indicated Mean Effective Pressure
IVO
Intake Valve Opening
LCV
Lower Calorific Value
MBT
Maximum Brake Torque
MFB
Mass Fraction Burned
NO_x
Nitrogen Oxides
RON
Research Octane Number
SI
Spark-Ignition
SOI
Start of Injection
TDC
Top Dead Centre
ULG
Unleaded Gasoline